Induced magnetism of oxygen in surfactant-grown Fe, Co, and Ni monolayers

C. Sorg,* N. Ponpandian, M. Bernien, K. Baberschke, and H. Wende
Institut für Experimentalphysik, Freie Universität Berlin, Arnimallee 14, D-14195 Berlin-Dahlem, Germany

R. Q. Wu
Department of Physics and Astronomy, University of California, Irvine, California 92697, USA
(Received 14 September 2005; revised manuscript received 21 December 2005; published 8 February 2006)

The well-known improvement of the layer-by-layer growth of ultrathin films of 3*d* ferromagnets by O surfactant is used to study the influence on their magnetism. X-ray magnetic circular dichroism (XMCD) reveals an induced magnetic moment of the O surfactant aligned in parallel to the 3*d* magnetization. In conjunction with density functional calculations we study the systematics of the x-ray absorption spectroscopy and XMCD at the O *K* edge.

DOI: 10.1103/PhysRevB.73.064409 PACS number(s): 75.70.−i, 78.70.Dm

I. INTRODUCTION

Surfactant-assisted growth of nanoscale structures on surfaces is a well-established technique. Various elements like the heavy element lead[1] but also light elements such as atomic oxygen[2–11] are used to improve the growth mode of 3*d* ferromagnetic films on single-crystalline substrates toward a more layer-by-layer one. Tailoring the growth modes for these ultrathin films is crucial since the magnetic properties are highly sensitive to minimal structural changes: If the nearest-neighbor distance varies by 0.03–0.05 Å only, the magnetic anisotropy energy may change by 10^2–10^3.[12,13] In the past we studied the effect of surfactant oxygen on the magnetic properties of Ni films on Cu(100). We confirm here that in agreement with our previous results for the surfactant-assisted growth of Ni on Cu, oxygen also acts as a surfactant for Co and Fe films. The preparation procedure is schematically presented in Fig. 1: At first, the atomic oxygen is adsorbed onto a clean Cu(100) crystal. Then the Fe, Co, and Ni films are prepared on the reconstructed surface. All three metals grow more layer by layer than without O up to >15 monolayers (ML). The O atoms always "float" on top of the ferromagnetic films.

An interesting question is if the surfactant oxygen affects the magnetic properties of the films. Indeed, it was demonstrated that the magnetic anisotropy energy of Ni is significantly enhanced using this surfactant.[8,11] Theory reveals that the main influence of the surfactant O on the magnetic anisotropy is a decrease in the magnitude of the surface anisotropy.[8] By applying the element specificity of the x-ray magnetic circular dichroism (XMCD) technique we were even able to identify an induced moment in the surfactant oxygen.[9] In the present work, we extend these investigations to ferromagnetic Co and Fe films grown with the help of the oxygen surfactant to study the changes in a systematic manner. Furthermore, *ab initio* calculations of the O *K*-edge XMCD were carried out to understand the spectroscopic fine structures from a fundamental point of view.

The paper is structured as follows: Details of the experiments are given in Sec. II, the results are discussed in Sec. III, and finally compared to *ab initio* calculations in Sec. IV in order to draw conclusions about the electronic structure and the magnetic moments.

II. EXPERIMENTAL DETAILS

The preparation and measurements are carried out *in situ* (base pressure $p \leqslant 2\times10^{-10}$ mbar). The Cu(100) substrate was first cleaned by cycles of Ar^+ bombardment and subsequent annealing to ~800 K. Then, the oxygen-induced $(\sqrt{2}\times2\sqrt{2})R45°$ "missing-row" reconstruction was achieved by dosing 1200 Langmuir of O_2 at 500 K. The low-energy electron diffraction (LEED) patterns of the Cu(100) before and after oxygen dosage are shown on the left-hand side of Fig. 2. The white rectangles highlight the elementary cell of the pattern of the clean Cu crystal, thus revealing the extra spots which appear due to the O adsorption and the $(\sqrt{2}\times2\sqrt{2})R45°$ reconstruction of the Cu surface. Afterward, the Fe, Co, and Ni films are deposited by electron-beam evaporation from high-purity rods. The electron energy varies between 176 eV (Fe with O surfactant) and 217 eV (Cu with and without O), thus accounting for the slightly different sizes of the white rectangles in the different patterns.[14] The LEED patterns of the surfactant grown films exhibit a $c(2\times2)$ structure (lower row of Fig. 2) whereas a simple $p(1\times1)$ structure is determined without surfactant (upper row of Fig. 2). As we have shown earlier this can be taken as a first indication that the oxygen atoms are located in a fourfold hollow site with $c(2\times2)$ symmetry [see, e.g., the details in

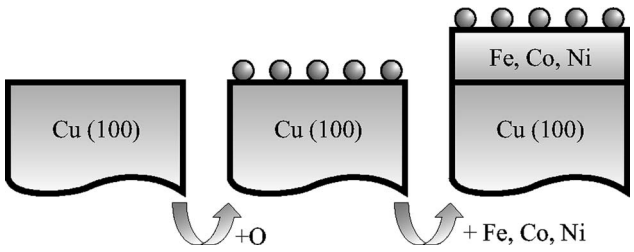

FIG. 1. Schematic illustration of the oxygen-surfactant-assisted growth of Fe, Co, and Ni films on Cu(100).

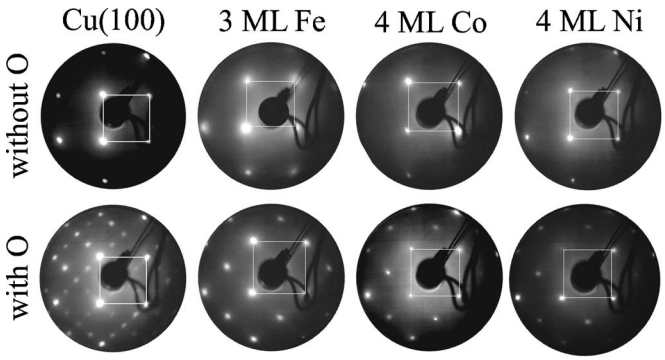

FIG. 2. LEED patterns of the 3*d* ferromagnets grown on Cu(100) with and without oxygen as a surfactant. The white rectangles highlight the elementary cell of the pattern of the clean Cu crystal.

the case of Ni (Ref. 6)]. Earlier works—e.g., by Thomassen *et al.*[15]—report 4×1 and 5×1 structures in the LEED patterns of Fe/Cu(100) in the thickness range below 5 ML. In our LEED pattern of clean Fe/Cu(100) these superstructures are not visible. This may be due to reasons given in a recent work by Bernhard *et al.*[16] who found that the reconstruction is not necessarily visible on very flat and clean substrates.

To confirm the improved growth by the help of the surfactant oxygen, medium-energy electron diffraction (MEED) oscillations were measured during evaporation. As shown in Fig. 3 these MEED oscillations are quite prominent up to thicknesses of 15 ML (Fe, Ni) and 25 ML (Co) for the growth of all films with the surfactant, whereas the oscillations clearly fade away starting from about 7 ML (Fe, Ni) and 17 ML (Co) for the bare films. The MEED intensity and the oscillatory amplitude strongly decrease for Fe/Cu(100) above 10 ML without surfactant (not shown in Fig. 3) as reported by Thomassen *et al.*,[15] whereas we do not find this behavior using the surfactant. This is an indication that the surfactant helps Fe to stay in an fct structure above 10 ML (see also Refs. 4, 17, and 18) whereas a transition from fct to bcc is determined in this thickness regime for the clean film.[15] The MEED oscillations of clean Fe on Cu(100) only start to be regular above 4 ML which reflects the complex growth and structure of Fe below this limit reported in the literature.[15,17,18] Various materials have proven to serve as surfactants and promote regular MEED oscillations from the beginning.[17,18] In the case of Co a layer-by-layer growth on Cu(100) accompanied by regular MEED oscillations has been reported for a long time.[19] The growth of Co on Cu(100) with O surfactant has to the best of our knowledge not been reported yet. Our MEED oscillations suggest that also in this case the layer-by-layer growth starts from the second ML. Only the growth of Co on the more anisotropic Cu(110) surface where the O surfactant works highly efficiently has already been reported.[20] The results of our present MEED experiment of Ni/Cu(100) with and without O are identical to our earlier results.[5]

The x-ray absorption spectroscopy (XAS) measurements are performed at the undulator beamline UE56/2-PGM2 at BESSY, the synchrotron radiation facility in Berlin, Germany. We determine the total electron yield by measuring the

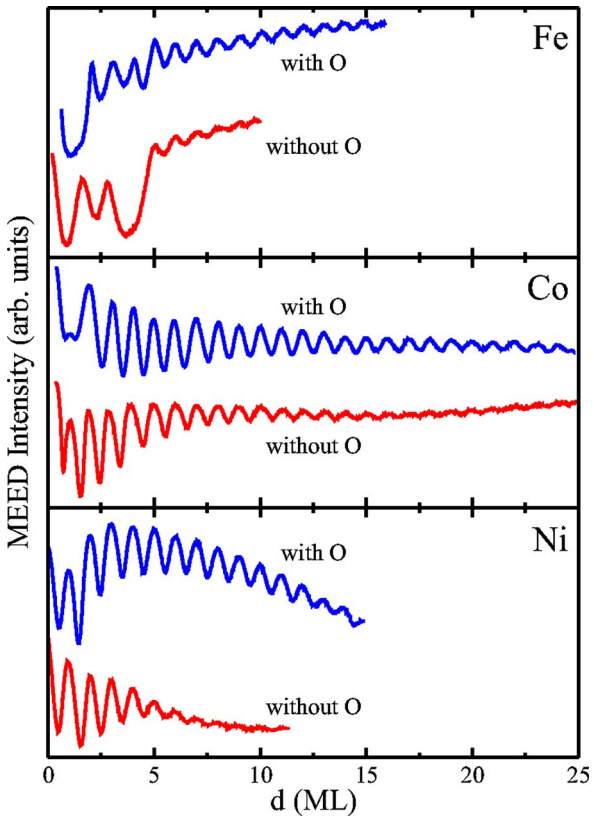

FIG. 3. (Color online) MEED oscillations of the 3*d* ferromagnets Fe, Co, and Ni grown on Cu(100) with and without oxygen as a surfactant.

drain current of the sample. An extraction grid (+1000 V) is mounted in front of the sample to avoid an artificial background when the dichroic spectra are measured in an applied magnetic field. The XMCD spectra are obtained (i) by reversing the magnetization of the films and (ii) by changing the helicity of the incoming photons. Thereby, additional artifacts in the XMCD spectra can be ruled out. The XMCD measurements are carried out on 3-ML Fe, 4-ML Co, and 15-ML Ni films. Since the easy axis of magnetization is normal to the plane for these Fe and Ni films and in plane for the Co film, the spectra are measured at normal x-ray incidence and at grazing incidence ($\varphi=20^{\circ}$), respectively. The spectra were taken in the gap-scan mode, which drives the undulator and monochromator simultaneously such that the energy picked by the monochromator and the maximal intensity emitted by the undulator coincide. This allowed us to measure the XMCD with a high brilliance and constant degree of circular polarization. Thereby, even the tiny XMCD signal at the O *K* edge could be clearly identified which reveals an induced magnetic moment in the surfactant.

To determine the nearest-neighbor distance R_{nn} of the O atoms to the Ni atoms of the topmost layer we have analyzed the surface-extended x-ray absorption fine structure (SEXAFS) at the O *K* edge of 15 ML Ni grown with O surfactant on Cu(100). The SEXAFS oscillations $k\chi(k)$ at 300 K and normal x-ray incidence are plotted in Fig. 4(a). Already in this figure it is obvious that the SEXAFS is mainly determined by a single frequency corresponding to

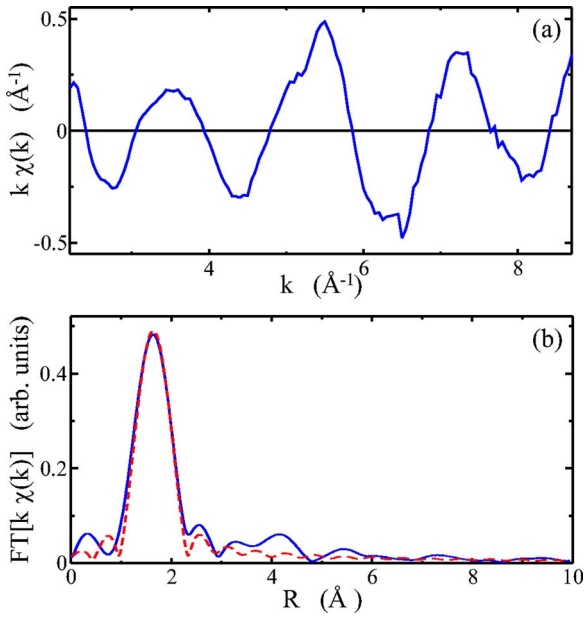

FIG. 4. (Color online) (a) O K-edge SEXAFS oscillations $k\chi(k)$ (300 K, normal x-ray incidence) and (b) the corresponding Fourier transform $|\mathrm{FT}[k\chi(k)]|$ of a 15 ML Ni film grown with O surfactant on Cu(100) as obtained from the experiment (solid line) and the fitting results on the nearest neighbor scattering shell (dashed line).

R_{nn}. This is seen even clearer in the corresponding Fourier transform $|\mathrm{FT}[k\chi(k)]|$ of the SEXAFS wiggles presented in Fig. 4(b). The nearest-neighbor distance was determined by fitting the data [FEFFIT (Ref. 21)] with a theoretical standard calculated with the FEFF8 code.[22] The experimental results are given as the solid line. The dashed line represents the FEFFIT result for the nearest-neighbor scattering shell. We find experimentally a nearest-neighbor O-Ni distance of $R_{nn}=(1.85\pm0.03)$ Å. Under the assumption that the tetragonal Ni film adopts the Cu in-plane lattice constant, from R_{nn} a height $h=0.41$ Å of the oxygen atoms above the first Ni layer can be determined. These results agree quite well with theoretical calculations of the geometric structure presented earlier[6] and in the present work (see below). This experimental determination of the local structure is quite helpful since it turns out that the size of the magnetic moments of the Ni atoms on the surface and also the induced moment in the surfactant oxygen sensitively depend on the height h as is discussed in Sec. IV.

III. RESULTS AND DISCUSSION

The advantage of measurements in the soft x-ray range is that the O K edge as well as the $L_{2,3}$ edges of the 3d ferromagnets Fe, Co, and Ni are located in this regime. Both the induced magnetism in the surfactant and the magnetic properties of the ferromagnetic films can be probed by measuring the XAS and XMCD as shown in Fig. 5 for the case of Co. A clear XMCD signal at the Co $L_{2,3}$ edges is determined but also a tiny XMCD signal at the O K edge can be revealed. Due to the excellent performance of the beamline, this oxygen signal of about 8% normalized to the small oxygen edge

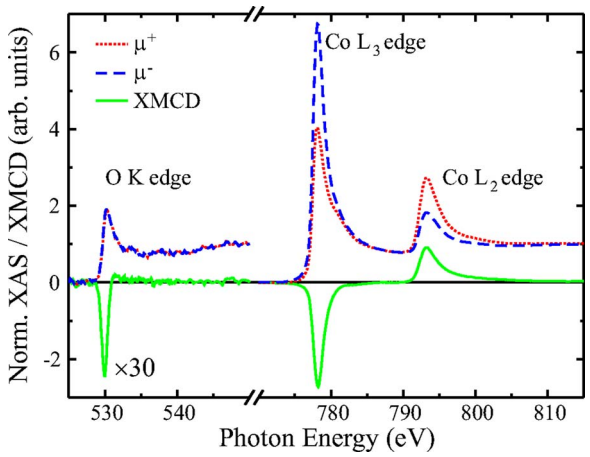

FIG. 5. (Color online) X-ray absorption coefficient and XMCD at the O K edge and Co $L_{2,3}$ edges for the surfactant-grown Co film.

jump (jump ratio $J_r=6\%$) can be revealed. The appearance of this signal shows that indeed the Co film induces a magnetic moment in the surfactant oxygen. However, one has to keep in mind that with XMCD at K edges only the orbital moment μ_L is probed.[9] The XMCD at the O K edge is much sharper [about 1 eV full width at half maximum (FWHM)] compared to the Co signal. This is a first indication that only the O $2p_z$ orbitals are polarized which hybridize with the Co 3d band. This is because the sharp structure located at 530 eV exactly originates from these hybridized $2p_z3d$ states.[23] Furthermore, the excellent statistics even allow for the identification of a small asymmetry in the O XMCD—i.e., the small positive contribution located at about 532 eV.

For the investigation of systematic trends we carried out these measurements for Fe, Co, and Ni films. We start the discussion with the analysis of the angular-dependent near-edge x-ray absorption fine structure (NEXAFS) spectra presented in Fig. 6. The NEXAFS of Co was recorded with linearly polarized x rays, the $\vec{E}$ vector aligned perpendicular to the [011] direction. In the case of Ni and Fe the isotropic XAS which is the average of the XAS recorded with circular-polarized light of the two helicities is shown. The clear angular dependence of the spectra for all 3d films clearly shows that (i) no bulklike oxide with the 3d elements is formed and (ii) the oxygen atoms "float" to the top of the surface. If the oxygen atoms were incorporated into the film, the angular dependence would be negligible because of the high symmetry. In contrast, on the surface the individual oxygen orbitals can be investigated. The spectra show quite similar trends for the three films: A sharp peak located at 530 eV displays the hybridized oxygen $2p_z$-3d metal states. Therefore, this peak is prominent at grazing x-ray incidence and decreases at normal x-ray incidence. The second structure at 538 eV originates from transitions to the hybridized O $2p_{xy}$-orbital–3d-metal 4sp bands. It is strong only in the normal-incidence geometry where $\Delta m=\pm1$. For p_z states $m=0$ and hence the p_z state does not respond to normal-incident light with circular polarization. Therefore, the opposite angular dependence is observed in comparison to the 530-eV structure. The broad peak at 550 eV stems from the scattering of the photoelectron at the nearest-neighbor 3d

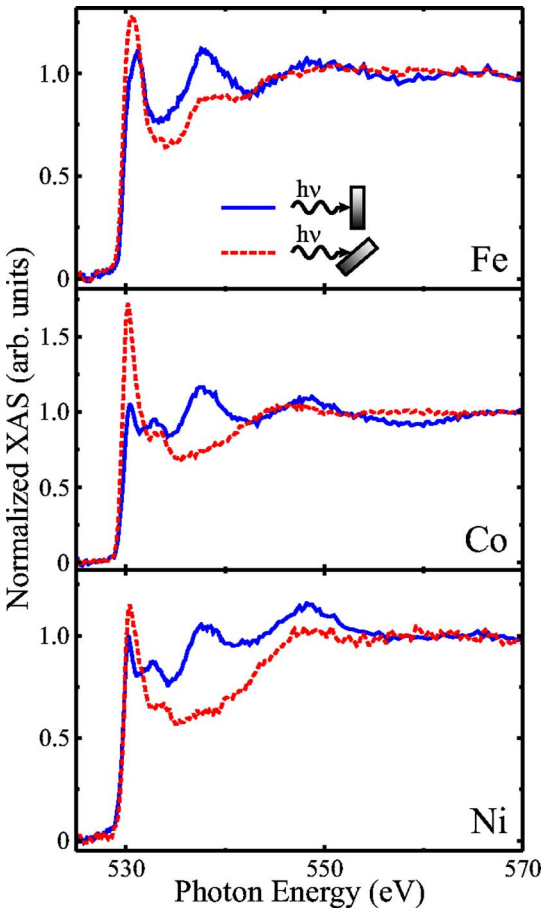

FIG. 6. (Color online) Angular-dependent NEXAFS at the O *K* edge of the 3*d* ferromagnets grown on Cu(100) with oxygen as a surfactant.

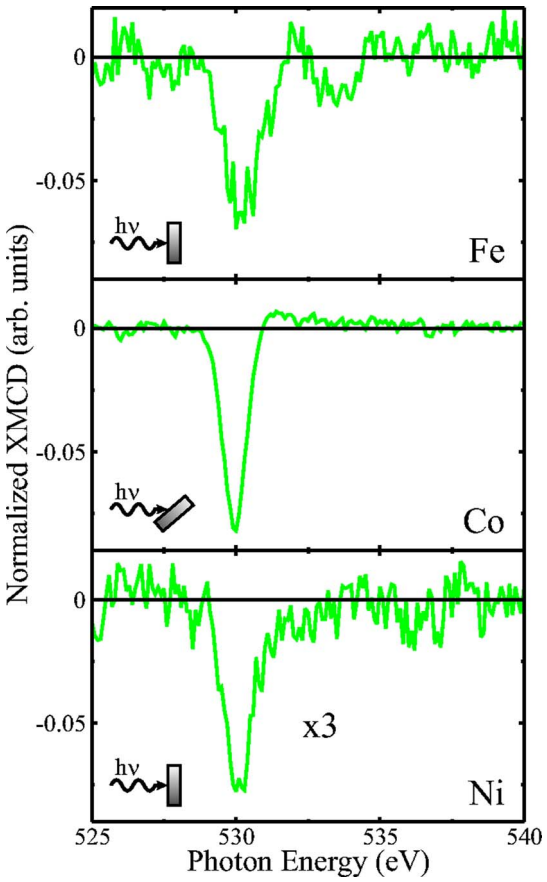

FIG. 7. (Color online) XMCD at the O *K* edge of the 3*d* ferromagnets grown on Cu(100) with oxygen as a surfactant.

metal atoms—hence, this feature can be assigned to the first EXAFS wiggle. Since quite similar spectral features and angular dependences are determined as seen in Fig. 6, we conclude that the local geometry and the local bonding of the surfactant oxygen atom to the 3*d* metal atoms is alike for the three films.

Turning to the dichroic spectra shown in Fig. 7 we find similar trends: All the XMCD spectra exhibit a sharp dichroic contribution at 530 eV. This negative contribution reveals that the induced orbital moment is aligned parallel to the spin and orbital moments of the ferromagnetic films (in agreement with Ref. 3). Since no XMCD signal is determined at 538 eV, we conclude that for all films the O $2p_z$ are magnetically polarized. Furthermore, the largest signal is found for Co and the smallest one for the Ni case. For the analysis of this behavior two effects have to be taken into account: On the one hand, one would expect that the magnetic moment of film determines the size of the induced moment. Therefore, one would expect the largest signal for Fe (bulk: $\mu_{\text{tot}}=2.1\mu_B$/atom) followed by Co (bulk: $\mu_{\text{tot}}=1.6\mu_B$/atom) and Ni (bulk: $\mu_{\text{tot}}=0.6\mu_B$/atom). On the other hand, only the O $2p_z$ orbitals are polarized which are probed stronger at grazing x-ray incidence (see Fig. 6). Since the Co film is magnetized in the film plane, the sample is measured at grazing incidence and therefore the largest O *K*-edge XMCD is determined for this case, followed by Fe and Ni (note the enlargement factor for Ni), which are measured at normal x-ray incidence. The shape of the O *K*-edge XMCD spectra compares well to the ones reported in literature for atomic oxygen on Co films[24] and molecular CO on Ni (Ref. 25) and Co (Ref. 26) films. Similarly sharp dichroic features are reported in reflectance at the carbon *K* edge of Fe/C multilayers.[27] Interestingly, for the CO molecules the XMCD is located directly at the π^* resonance.

IV. COMPARISON TO THEORY

Density functional calculations for O adsorption on fcc Fe(100), Co(100), and Ni(100) surfaces were conducted using the thin-film full potential linearized augmented plane wave (FLAPW) method.[28] To mimic the experimental condition, we placed a $c(2\times2)$ oxygen layer on top of a seven-layer slab of 3*d* atoms. The lattice size in the lateral plane is fixed at that of bulk Cu ($a=3.61$ Å), whereas the vertical positions of all atoms are optimized through the energy minimization procedure guided by atomic forces calculated from first principles. No shape approximation was assumed in charge, potential, and wave function expansions. The core states were treated fully relativistically while the spin-orbit interaction among valence states was invoked second-variationally in the charge self-consistence loop. Both the local density approximation (LDA, in the formula of Hedin

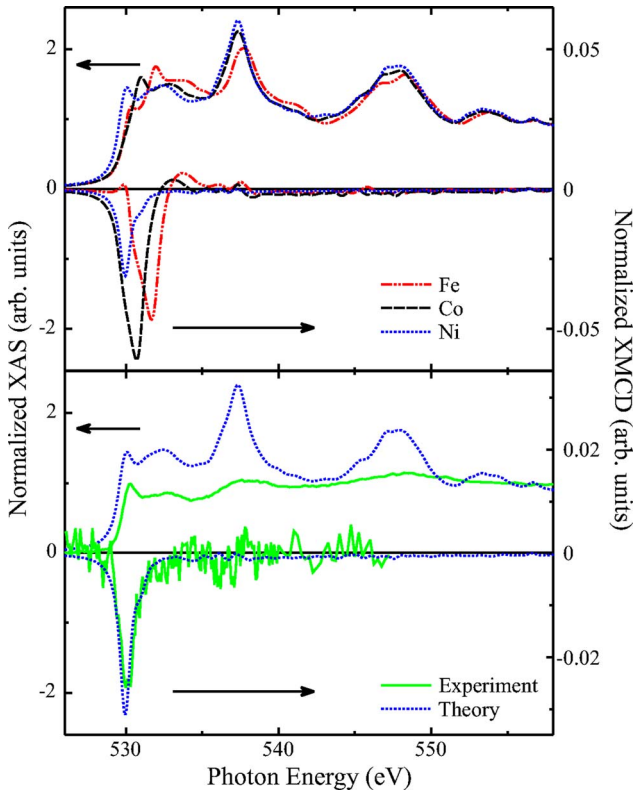

FIG. 8. (Color online) Top: calculated XAS and XMCD spectra of the O adatom on the fcc Fe(100) (dash–double-dotted line), Co(100) (dashed line), and Ni(100) (dotted line) films for the normal incidence geometry. Bottom: comparison of measured (solid line) and calculated (dotted line) XAS and XMCD of the O adatom on the Ni(100) film at normal incidence. Note that there is no scaling factor between experiment and calculation. The scale of the XAS is given on the left-hand side, the one of the XMCD on the right-hand side.

and Lundqvist[29]) and the generalized gradient approximation (GGA, in the formula of Perdew, Burke, and Ernzerhof[30]) were adopted to describe the exchange-correlation interaction. Energy cutoffs of 256 Ry and 13 Ry were chosen for the charge-potential and basis expansions in the interstitial region. In the muffin-tin region, spherical harmonics with a maximum angular momentum quantum number of $\ell_{\max}=8$ were used.

The optimized distances between the oxygen adatom and its nearest Fe, Co, and Ni neighbors are 1.85–1.86 Å from LDA calculations and 1.93 Å from GGA calculations. The LDA results agree with our SEXAFS data very well and are employed for other comparisons henceforth. It is known that the GGA overestimates the lattice sizes of oxides, and here we find it does so also for surface problems. Nevertheless, we use GGA to optimize the positions of the substrate 3*d* atoms, for which the gradient corrections are crucial. The presence of O produces sizable bulking reconstructions in the subsurface layer. For example, the subsurface Fe atom right beneath the O adatom goes inwards by 0.08 Å in O/Fe(100), whereas the other Fe atom remains at its bulk position. The interlayer distance between adjacent 3*d* layers is 1.73–1.75 Å, a result that agrees with the experiment.

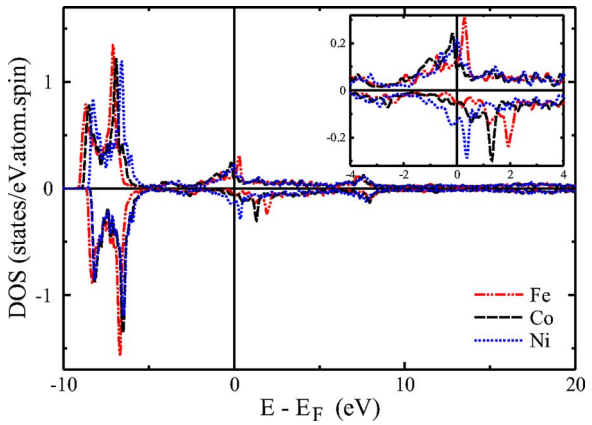

FIG. 9. (Color online) Calculated density of O *p* states. Positive and negative values represent states in the majority- and minority-spin channels, respectively. Zero energy indicates the position of the Fermi level. The inset gives an enlarged view for states around E_F.

The calculated spin magnetic moments projected into the O muffin-tin sphere ($r=0.74$ Å) are $0.053\mu_B$, $0.132\mu_B$, and $0.053\mu_B$ in O/Fe(100), O/Co(100), and O/Ni(100), respectively. Their orbital moments are very small, $0.0024\mu_B$, $0.0047\mu_B$, and $0.0021\mu_B$. The O adatoms significantly reduce the magnetization of the surface 3*d* atoms. Particularly, the spin magnetic moment of the surface Ni atom is only $0.26\mu_B$, much smaller than those of the interior Ni atoms, $0.66\mu_B$–$0.69\mu_B$. It is important to note that the spin and orbital magnetic moments of both O and surface Fe, Co, and Ni atoms strongly depend on the relaxation of the oxygen atom.[31]

The calculated XAS and XMCD spectra for the normal incidence geometry are presented in Fig. 8, accompanied by the experimental data for O/Ni(100). Note that (i) only the dipole transitions are treated in our calculations, (ii) the spectra are convoluted by Doniach-Sunjic shapes of 0.45 eV wide for lifetime broadening,[32] and (iii) theoretical spectra are shifted by 25 eV in energy to accommodate the core-hole relaxation effect. Intriguingly, all the spectroscopic features, including the peak structures and the XMCD/XAS ratio, are satisfactorily reproduced. Note also that there is no free scaling factor between experiment and theory. This indicates that the model used in the calculations represents the atomic arrangements in experimental samples very well. The XMCD spectra also depend sensitively on the height of oxygen adatom on the substrates. The XMCD peak calculated with the GGA structure is about 1.5 times stronger than that shown in Fig. 8. The agreement of the XMCD spectrum confirms that one should use 1.85–1.86 Å for the O 3*d* bond length. Furthermore, as was also demonstrated in most other cases, the core-hole relaxation does not significantly affect the profile of the XAS and XMCD.[33]

Despite the fact that the spin and orbital magnetic moments of O are small, the XMCD signals are sizable at the threshold for all three systems. In the plot of the density of states (DOS) with the O 2*p* features shown in Fig. 9, it is clear that these XMCD peaks stem from the substrate-induced states right above the Fermi level. As displayed in Figs. 9 and 10, these are the tails of the substrate states. They

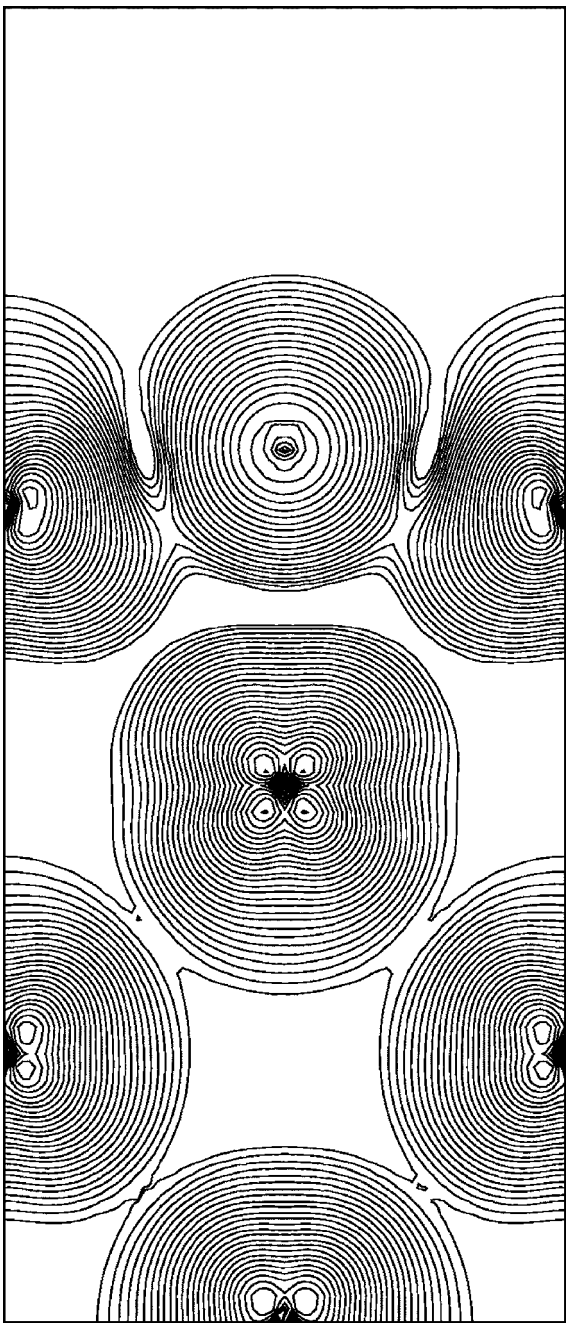

FIG. 10. Energy-sliced charge density from states between 0.1 and 0.7 eV above E_F for O/Ni(100). Contours shown in the (100) plane start from $1.0\times10^{-4}e$/a.u.^{3} and increase successively by a factor of 1.2.

show a strong spin polarization and have an imbalance in the $m=1$ and $m=-1$ compositions in their wave functions. This is mainly because of the large spin orbit coupling inherited from the substrate atoms. It is interesting to note that the positions of these states shift to the high-energy side in a sequence as O/Ni(100), O/Co(100), and O/Fe(100). This is reflected in the XAS and XMCD calculated for the three systems. Probably due to the wider lifetime and experimental broadening, one needs to be more attentive to find these shifts in our experimental data [cf. the difference between data for O/Fe(100) and O/Ni(100)].

The other two main peaks in Fig. 9, 7–8 eV and 17–19 eV above E_F, show very small exchange splitting and weak resonance with the substrate states. Subsequently, they are only detected in the XAS but not in XMCD. Theoretical calculations confirmed that the states 7–8 eV above E_F are $p_{x,y}$ features, as deduced from the dependence of intensity on the angle of incidence.

V. SUMMARY

We used the well-known improvement of layer-by-layer growth of Fe, Co, and Ni by O surfactant to study the modification of the element-specific magnetization. Angular-dependent NEXAFS measurements at the O *K* edge give final evidence that (i) the oxygen does not form a bulklike oxide with the 3*d* ferromagnet and (ii) the O atoms stay on top of the growing film. Due to the hybridization with the ferromagnetic film, the O atoms acquire an induced magnetic moment that can be probed by XMCD at the O *K* edge. Since the initial states of XAS at the O *K* edge are not spin-orbit split, only the orbital moment is probed by XMCD at the O *K* edge. In conjunction with density functional calculations using the thin-film full-potential linearized augmented plane-wave method we have studied the systematics of the XAS and XMCD at the O *K* edge. The calculations reproduce the experimental results very well. No scaling factor occurs between the two. We could show that all the spectral features can be identified with the help of the calculations. Finally, theory reveals spin and orbital moments of the ferromagnetic films as well as the induced moments of the oxygen surfactant.

ACKNOWLEDGMENTS

We thank A. Scherz for his contribution in the early state of this work as well as H. Ebert and V. Popescu for helpful discussions. We acknowledge the BESSY crew for their technical support, in particular F. Senf. Support by BMBF (05 KS4 KEB/5) is gratefully acknowledged.

*Corresponding author. FAX: +49 30 838-53646. Electronic address: babgroup@physik.fu-berlin.de; URL: http://www.physik.fu-berlin.de/~bab/

[1] J. Camarero, T. Graf, J. J. de Miguel, R. Miranda, W. Kuch, M. Zharnikov, A. Dittschar, C. M. Schneider, and J. Kirschner, Phys. Rev. Lett. **76**, 4428 (1996).

[2] W. F. Egelhoff, Jr., P. J. Chen, C. J. Powell, M. D. Stiles, R. D. McMichael, J. H. Judy, K. Takano, and A. E. Berkowitz, J. Appl. Phys. **82**, 6142 (1997).

[3] F. Bisio, R. Moroni, M. Canepa, L. Mattera, R. Bertacco, and F. Ciccacci, Phys. Rev. Lett. **83**, 4868 (1999).

[4] L. Li, A. Kida, M. Ohnishi, and M. Matsui, Surf. Sci. **493**, 120

(2001).
[5] J. Lindner, P. Poulopoulos, R. Nünthel, E. Kosubek, and K. Baberschke, Surf. Sci. **523**, L65 (2003).
[6] R. Nünthel, T. Gleitsmann, P. Poulopoulos, A. Scherz, J. Lindner, E. Kosubek, Ch. Litwinski, Z. Li, H. Wende, K. Baberschke, S. Stolbov, and T. S. Rahman, Surf. Sci. **531**, 53 (2003).
[7] R. Nünthel, J. Lindner, P. Poulopoulos, and K. Baberschke, Surf. Sci. **566-568**, 100 (2004).
[8] J. Hong, R. Q. Wu, J. Lindner, E. Kosubek, and K. Baberschke, Phys. Rev. Lett. **92**, 147202 (2004).
[9] C. Sorg, N. Ponpandian, A. Scherz, H. Wende, R. Nünthel, T. Gleitsmann, and K. Baberschke, Surf. Sci. **565**, 197 (2004).
[10] M. Farle, Surf. Sci. **575**, 1 (2005).
[11] T. Nakagawa, H. Watanabe, and T. Yokoyama, Phys. Rev. B **71**, 235403 (2005).
[12] O. Hjortstam, K. Baberschke, J. M. Wills, B. Johansson, and O. Eriksson, Phys. Rev. B **55**, 15026 (1997).
[13] P. Poulopoulos and K. Baberschke, J. Phys.: Condens. Matter **11**, 9495 (1999).
[14] Since the LEED system is not the key component of the UHV chamber, the sample cannot be perfectly aligned with respect to the LEED screen because of geometrical constraints by other equipment. Thus, a nonperfectness of the spots (symmetry, brightness, etc.) and high electron energies occur.
[15] J. Thomassen, F. May, B. Feldmann, M. Wuttig, and H. Ibach, Phys. Rev. Lett. **69**, 3831 (1992).
[16] T. Bernhard, M. Baron, M. Gruyters, and H. Winter, Phys. Rev. Lett. **95**, 087601 (2005).
[17] A. Kirilyuk, J. Giergiel, J. Shen, and J. Kirschner, Phys. Rev. B **52**, R11672 (1995).
[18] A. Kirilyuk, J. Giergiel, J. Shen, M. Straub, and J. Kirschner, Phys. Rev. B **54**, 1050 (1996).
[19] J. J. de Miguel, A. Cebollada, J. M. Gallego, S. Ferrer, R. Miranda, C. M. Schneider, P. Bressler, J. Garbe, K. Bethke, and J. Kirschner, Surf. Sci. **211-212**, 732 (1989).
[20] C. Tölkes, R. Struck, R. David, P. Zeppenfeld, and G. Comsa, Phys. Rev. Lett. **80**, 2877 (1998).
[21] M. Newville, B. Ravel, D. Haskel, J. J. Rehr, E. A. Stern, and Y. Yacoby, Physica B **208/209**, 154 (1995).
[22] A. L. Ankudinov, B. Ravel, J. J. Rehr, and S. D. Conradson, Phys. Rev. B **58**, 7565 (1998).
[23] F. May, M. Tischer, D. Arvanitis, M. Russo, J. Hunter-Dunn, H. Henneken, H. Wende, R. Chauvistré, N. Mårtensson, and K. Baberschke, Phys. Rev. B **53**, 1076 (1996).
[24] K. Amemiya, T. Yokoyama, Y. Yonamoto, D. Matsumura, and T. Ohta, Phys. Rev. B **64**, 132405 (2001).
[25] T. Yokoyama, K. Amemiya, M. Miyachi, Y. Yonamoto, D. Matsumura, and T. Ohta, Phys. Rev. B **62**, 14191 (2000).
[26] K. Amemiya, T. Yokoyama, Y. Yonamoto, M. Miyachi, Y. Kitajima, and T. Ohta, Jpn. J. Appl. Phys., Part 2 **39**, L63 (2000).
[27] H.-Ch. Mertins, S. Valencia, W. Gudat, P. M. Oppeneer, O. Zaharko, and H. Grimmer, Europhys. Lett. **66**, 743 (2004).
[28] E. Wimmer, H. Krakauer, M. Weinert, and A. J. Freeman, Phys. Rev. B **24**, 864 (1981); M. Weinert, E. Wimmer, and A. J. Freeman, *ibid.* **26**, 4571 (1982).
[29] L. Hedin and B. I. Lundqvist, J. Phys. C **4**, 2064 (1971).
[30] J. P. Perdew, K. Burke, and M. Ernzerhof, Phys. Rev. Lett. **77**, 3865 (1996); J. P. Perdew, K. Burke, and Y. Wang, Phys. Rev. B **54**, 16533 (1996).
[31] In our previous publication (Ref. 8) only the GGA was applied, yielding spin and orbital magnetic moments of O in O/Ni(100) of $0.17\mu_B$ and $0.0025\mu_B$, respectively. The spin magnetic moment of the surface Ni in O/Ni(100) with the GGA structure becomes $0.77\mu_B$, even larger than those in the bulk region.
[32] S. Doniach and M. Sunjic, J. Phys. C **3**, 285 (1970).
[33] R. Q. Wu, Phys. Rev. Lett. **94**, 207201 (2005).